# BioMoSS: ROS-generating Photocatalysts for the Disinfection of Potable Water Systems

John Abdou[1], John Vance[2], Anna Lu[3]
*KBR, Moffett Field, CA, 94035*

*and*

Lance Delzeit[4]
*NASA Ames Research Center, Moffett Field, CA, 94035*

**With NASA's desire to replace iodine as the biocide within the potable water system of future missions, we continue our development of the biocidal $MoS_2$ (BioMoSS) system. BioMoSS is a visible-light activated photocatalyst based upon few-layered vertically aligned molybdenum disulfide (FLV-$MoS_2$) for the production of reactive oxygen species (ROS) as a biocide. FLV-$MoS_2$ has been reported to have a high bacterial kill rate. We report significant improvements in the vertical-alignment and biocidal efficacy of the FLV-$MoS_2$ compared to our initial results reported last year. Furthermore, we report the results of peroxide formation with and without surface deposition using gold. Finally, we investigate the delamination of the FLV-$MoS_2$ films under immersion in water.**

## Nomenclature

| | | |
|---|---|---|
| *AU* | = | absorbance units |
| *BioMoSS* | = | biocidal molybdenum disulfide |
| *CFU* | = | colony forming unit |
| *DI* | = | deionized |
| *FLV-$MoS_2$* | = | few-layered vertically aligned molybdenum disulfide |
| *$H_2O_2$* | = | hydrogen peroxide |
| *IBS* | = | ion beam sputtering |
| *kV* | = | killivolts |
| *μM* | = | micromolar |
| *μL* | = | microliter |
| *mA* | = | milliamperes |
| *mM* | = | millimolar |
| *mL* | = | milliliter |
| *Mo* | = | molybdenum |
| *$MoS_2$* | = | molybdenum disulfide |
| *nm* | = | nanometer |
| *ROS* | = | reactive oxygen species |
| *SCCM* | = | standard cubic centimeter per minute |
| *SEM* | = | scanning electron microscopy |
| *$SiO_2$* | = | silicon dioxide |
| *TEM* | = | transmission electron microscopy |
| *UV* | = | ultraviolet |

[1] Research Scientist, Bioengineering Branch, and Mail Stop 239-15.
[2] Research Engineer, Bioengineering Branch, and Mail Stop 239-15.
[3] Associate Scientist, Bioengineering Branch, and Mail Stop 239-15.
[4] Physical Scientist, Bioengineering Branch, and Mail Stop 239-15.

## I. Introduction

WITH renewed interest in human exploration beyond low-Earth orbit, there has been an increased demand for technological advances in environmental control and life support systems. The opposing requirements of dramatically increased duration/reliability and reduced system mass/complexity require novel solutions in such systems. Of key importance is the recycling, storage, and residual disinfection of crew potable water. Traditional means of water disinfection employ minute additions of biocidal agents (e.g. iodine, silver, bleach, etc.) by means of chemical dosing or electrodissolution of metal.[1-5] While the biocidal efficacies of such agents are well-proven, there are numerous potential alternatives of interest reported in literature without requiring an in-line filtration system or a water system with compatible materials.

In the past several years, increasing attention has been given to the photochemical production of biocidal agents at the water/semiconductor interface. Through the reduction of dissolved oxygen and oxidation of water, photo-excited semiconductors with appropriate band structures and surface chemistry produce reactive oxygen species (ROSs), including hydrogen peroxide ($H_2O_2$), hydroxyl radicals, superoxide radicals, and singlet oxygen. At and inside the cell membrane, these ROSs can inactivate microbes.

One of the most promising materials for this application is few-layered vertically aligned molybdenum disulfide (FLV-$MoS_2$), which was synthesized and characterized by the Cui Group at Stanford.[6,7] FLV-$MoS_2$ is a nanomaterial grown by the sulfurization of a thin molybdenum (Mo) metal film.[7] Under appropriate growth conditions, sulfurization results in small, vertically-aligned grains, rather than basally-oriented stacked planes. This has been explained by the relative facility of sulfur diffusion in the van der Waals gap (between the layers)[6] to that in Mo metal at elevated temperature and the relaxation of stress, generated by volume expansion, into the free surface of the film.[8] This results in a widened band-gap, shifted in the visible range, capable of driving photochemical ROS generation at exposed (high energy) dangling bond edge sites shown schematically in the previous paper.[9] The combination of photochemically-compatible band structure and high surface activity makes FLV-$MoS_2$ a highly effective material for the inactivation of microbes in water with a kill efficacy reported to be >99.999% under exposure to visible light with intensities similar to that of sunlight on the order of 60 minutes.[7]

Most previous work has tested the biocidal efficacy of FLV-$MoS_2$ and other similar materials in static conditions such as in beakers or other similar configurations. The goal of the BioMoSS project is to translate these results into a flow cell configuration with conditions similar to those found in the humidity condensate system of a crewed spacecraft.* In this continuing work, optimal FLV-$MoS_2$ growth conditions were investigated and evaluated by peroxide formation and biocidal efficacy testing to obtain an effective photodisinfection technology for spacecraft potable water systems. This work reports increased FLV-$MoS_2$ vertical-alignment to over 90% estimated from visual observations of transmission electron microscopy (TEM) images as well as two broadly-absorbing peaks observed with UV-Vis spectroscopy inherent to $MoS_2$. With experiments in the positioning of the sulfur to cooler regions in the furnace, the photocatalytic performance of FLV-$MoS_2$ significantly increased to 1.5 µM $H_2O_2$ formed and 1.9 log kill in 4 hours. Decoration of the FLV-$MoS_2$ substrates with gold nanoparticles resulted in double the $H_2O_2$ formation rate with a 5 minute deposition time. Finally, the delamination of FLV-$MoS_2$ films in water was investigated with early findings that glassy carbon substrates prevented this film failure.

## II. Materials and Methods

### A. FLV-$MoS_2$ Synthesis and Characterization

The 2nd generation process, modified from earlier work,[9] is described here. Mo thin films (~10-30nm) sputtered by magnetron sputtering on quartz substrates (17 mm x 25 mm) were provided by Scientific Coating Labs. Sulfurization of the Mo thin film to produce $MoS_2$ was done in a 1 inch diameter quartz tube furnace (Lindbergh Blue M). 5 g of sulfur powder (99.998%, Sigma-Aldrich) was placed on the insulated edge of the tube furnace, such that sulfur vapor was carried through the tube to the Mo sample film at the heating center, which is the location of the thermocouple and the center of the furnace by distance. The quartz tube was sealed and put under vacuum with a base pressure of 1 Torr measured with a capacitance manometer (MKS AA01A13TBAS3B00000). Argon gas (ultra high purity, Matheson Tri-Gas) was flown through the system at a rate of 95 SCCM, giving a system pressure of approximately 3.5 Torr at the tube inlet. The system was purged of residual air and water vapor for 60 minutes by the argon flow. After the system purge, the system pressure was adjusted to the target reaction pressure (3.5-30 Torr) using a ball valve. The temperature was ramped linearly to the reaction temperature (450-600 °C) in 10 minutes and

* Introduction adapted from our previous ICES paper[9]

then held at temperature for 10 minutes. Heating was then stopped and the top of the tube furnace was opened to allow for a natural cool down.

FLV-$MoS_2$ samples were characterized with UV-Vis spectroscopy (Ultrospec 3300 pro) and transmission electron microscopy (TEM). The reacted quartz sample slide was placed perpendicular in the beam path and the absorbance measured from 200-1100 nm. The lattice structure of the reacted $SiO_2$ support film TEM grids were observed using a TEM (Hitachi H-9500) at 300 kV accelerating voltage and magnifications of 200,000 and 500,000X.

### B. Photocatalytic Performance

The FLV-$MoS_2$ substrate was placed film-side up at the bottom of a 50 mL Pyrex beaker, which was then filled with 25 mL of deionized (DI) water for $H_2O_2$ formation testing or 25 mL of an approximately $10^6$ colony forming units (CFU)/mL K12 *Escherichia coli* suspension in DI water for biocidal efficacy testing. The substrate-containing beaker and a control beaker containing DI water with no substrate are illuminated from above using a homemade illumination system employing LED flood lamps (Cree TPAR38-1503040FH25-12DE26-1) while an additional control beaker with DI water or bacteria suspension was kept in the dark as a dark control. Aliquots were taken after 2 and 4 hours for $H_2O_2$ formation or biocidal efficacy testing. The measurement taken at 4 hours was used as the primary metric since earlier studies showed 4 hours were required to produce a 1 log kill within a bacterial sample.[9] The distance from the light source to the FLV-$MoS_2$ was adjusted to ensure slightly greater than solar intensity in the visible wavelengths. The spectral intensity of the incident light at the $MoS_2$ was measured using a portable spectral light meter (Gigahertz-Optik, MSC15). As the light source does not produce significant ultraviolet (UV) radiation, no filter was necessary to prevent UV based biocidal activity in the tests.

$H_2O_2$ formation in deionized water can be measured colorimetrically using a modified ferrous oxidation in xylenol orange 1 assay.[10] A stock solution of 10 μM $H_2O_2$ was prepared from 30% $H_2O_2$ solution by serially diluting 1000X two times. The concentration of the $H_2O_2$ solution was confirmed with an absorbance measurement at 240 nm within 10% of 0.427 AU based on the absorption value calculated from the molar extinction coefficient in literature[11] using UV-Vis spectroscopy (Molecular Devices SpectraMax Plus). Calibration solutions ranging from 0.2 to 5 μM were prepared from the 10 μM $H_2O_2$ stock solution. The xylenol orange 1 assay reagents were made in two solutions: the first containing 2 mM xylenol orange and 2 M Sorbitol in water and the second of 5 mM ammonium ferrous sulfate and 500 mM sulfuric acid in water. 50 μL of each reagent solution was mixed with 1 mL of each calibration solution and each sample aliquot. The mixture was then vortex mixed for 3 seconds, allowed to react for 10 minutes, and measured for absorbance at 560 nm on the UV-Vis.

Biocidal efficacy was measured by CFU enumeration on agar plates. The CFUs in the dark and light controls and FLV-$MoS_2$ systems after light exposure were enumerated in triplicate by the single plate-serial dilution spotting method.[12] Each aliquot was serially-diluted (1:10) 5 times with DI water in a sterile 96-well plate. Each dilution had 20 μL drawn and deposited as a series of 25-30 microdroplets onto a section of an LB agar plate and incubated at 37 °C overnight. The viable CFUs grown under the FLV-$MoS_2$ are then counted and compared with the light control.

### C. Gold Deposition

FLV-$MoS_2$ samples made on quartz slides and TEM grids were deposited with gold using ion beam sputtering (IBS) system (South Bay Technology) using a 99.9% gold source with a base pressure of $6 \times 10^{-6}$ Torr. The operating pressure of the IBS was $1 \times 10^{-5}$ Torr. The samples sputtered at a rate of ~1 nm/min under a 6 mA current for 1-20 minutes.

### D. Film Delamination

FLV-$MoS_2$ samples made on quartz slides, glassy carbon plates, and silicon wafers were immersed in 25 mL of DI water for up to 2 weeks. Delamination was visually inspected on a weekly basis and observed by scanning electron microscopy (SEM, Hitachi S-4800) at 20 kV accelerating voltage at the end of the immersion period.

## III. Results and Discussion

### A. FLV-$MoS_2$ Synthesis and Characterization

Early FLV-$MoS_2$ samples were grown using Mo films deposited by in-house ion bean sputtering.[9] The samples grown from these depositions showed less than 50% vertical-alignment within the grown films. The FLV-$MoS_2$ growth described in the literature[6,7] used e-beam evaporation and magnetron sputtering to prepare the films. In order

to more closely replicate the Mo films produced within the literature[6,7], the Mo deposition using magnetron sputtering was outsourced to Scientific Coating Labs. Over the course of the research, four separate Mo film depositions were obtained with nominal thicknesses of 12.6, 13.8, 16.6, and 30.6 nm. The first deposition (12.6 nm) showed vertical-alignment up to 80%, depending on the processing conditions, with the best vertical-alignment observed at 20 Torr and 500 °C.

The second deposition (13.8 nm) also showed vertical-alignment up to 80%, with the best vertical-alignment at 30 Torr and 500 °C (Figure 1A). However, the $MoS_2$ made with the second deposition substrates had a reproducibility issue that was apparent in samples made under the same chemical vapor deposition processing conditions as seen in Figures 1A and 1B. This was partially due to visually non-uniform Mo film coatings observed in the second deposition. Furthermore, the lighter color of the second depositions indicates that the Mo film thickness may be less than that of the first deposition despite the 13.6 nm film thickness reported by Scientific Coating Labs. The Mo film thickness is known to affect the vertical-alignment of $MoS_2$ with thinner Mo films resulting in basal growth of the $MoS_2$. With a thicker, continuous Mo film, basal $MoS_2$ growth over a continuous film is not possible due to the high strain energy induced from large area basal planes. In order to relieve this strain energy, vertical-alignment growth is driven.[8] With a thinner, discontinuous Mo film, basal $MoS_2$ has room to grow outward. As a result, basal growth is promoted as the basal $MoS_2$ plane surface energy is two orders of magnitude lower than the edge sites in the vertically-aligned $MoS_2$.

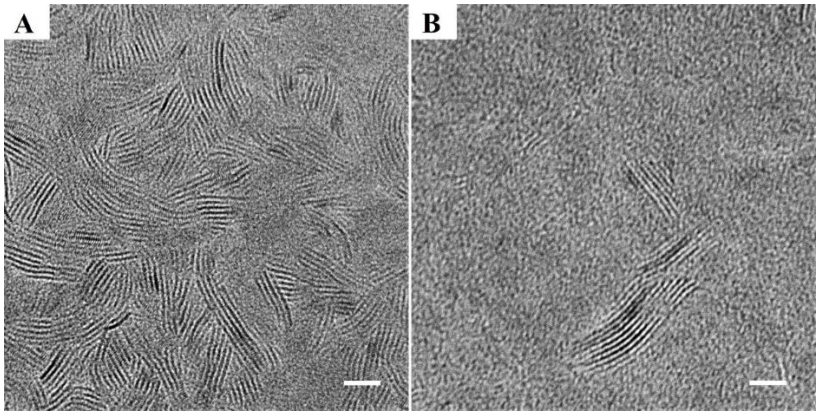


**Figure 1. High-resolution transmission electron micrographs of FLV-$MoS_2$ samples grown from the second Mo deposition with A) 80% vertical-alignment and B) 10% vertical-alignment at 500000X magnification. Both samples are on quartz slides grown at 500 °C and 30 Torr. Scale bars represent 5 nm.**

With the third deposition, the Mo films were made with 16.6 nm film thickness, which corrected this issue. The Mo film displayed visual improvements in the Mo film uniformity compared to the remaining substrates of the second deposition. As a result, the optimal temperature and processing conditions were re-investigated based on the results of BioMoSS experiments with the first two depositions as well as recommendations from one of the researchers who developed the technology. Various degrees of vertical-alignment were observed after FLV-$MoS_2$ growth at 30 Torr and 450-600 °C (Figure 2). At 30 Torr and 500 °C, TEM micrographs show greater than 90% vertical-alignment as seen in Figure 2B; this was a notable improvement over most of the previous results. At 550 °C and 600 °C, the vertical-alignment was still near 90% as seen in Figures 2C and 2D. When the reaction temperature was reduced to 450 °C, the vertical-alignment decreased to about 70% (Figure 2A). This agrees with what was reported in the literature[6-8] that cites 500 – 600 °C as the optimal growth temperature range.

From this re-investigation of the BioMoSS growth conditions with the thicker Mo thickness, the optimal conditions were determined as 30 Torr and 500 °C. At these conditions, the observed vertical-alignment (greater than 90%) with domains of 3-10 monolayers is similar to that reported in the literature,[7] as shown in Figure 3. The increased vertical-alignment over the first two depositions is due to increased Mo film thickness.

A fourth deposition was carried out with twice the thickness of the third deposition with the expectation that the higher seed layer thickness would further improve the vertical-alignment growth.[9] Two experiments were conducted to account for possible factors affecting FLV-$MoS_2$ based on discussions with one of the researchers who developed the technology.[13] The first experiment investigated the aging of the Mo films in relation to photocatalytic performance. It was reported in the literature[14] that Mo films were measured to have an initial native oxide layer of 1.1 nm thickness after deposition that continues to grow to 5.0 nm after 60 days and 6.7 nm after 116 days. The original disinfection research using FLV-$MoS_2$ was done immediately after Mo deposition. In order to investigate the performance of FLV-$MoS_2$ with minimal oxide layer growth, FLV-$MoS_2$ samples were prepared under optimal growth conditions within 2 days after the sputtering was completed. Further studies of the FLV-$MoS_2$ with the Mo films stored over time are ongoing. The second experiment assessed FLV-$MoS_2$ photocatalytic performance in relation to position in the furnace. The researcher of FLV-$MoS_2$ stated that high sulfur flux over the Mo film can result in sulfur passivation

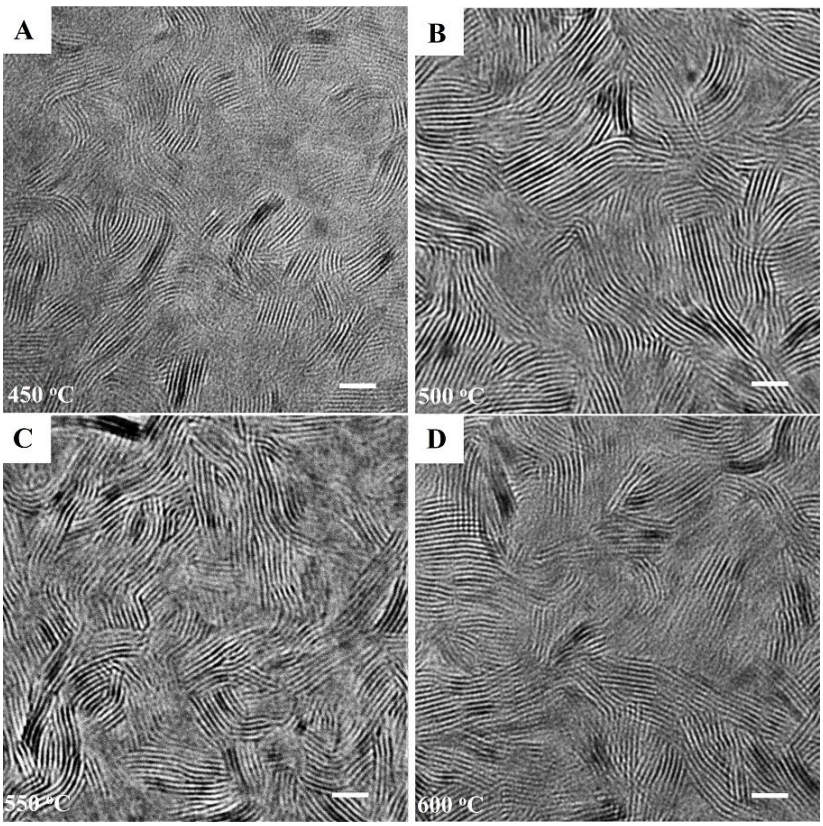


**Figure 2. High-resolution transmission electron micrographs of FLV-$MoS_2$ deposited at: A) 450 °C, B) 500 °C, C) 550 °C, and D) 600 °C at 30 Torr. Scale bars represent 5 nm.**

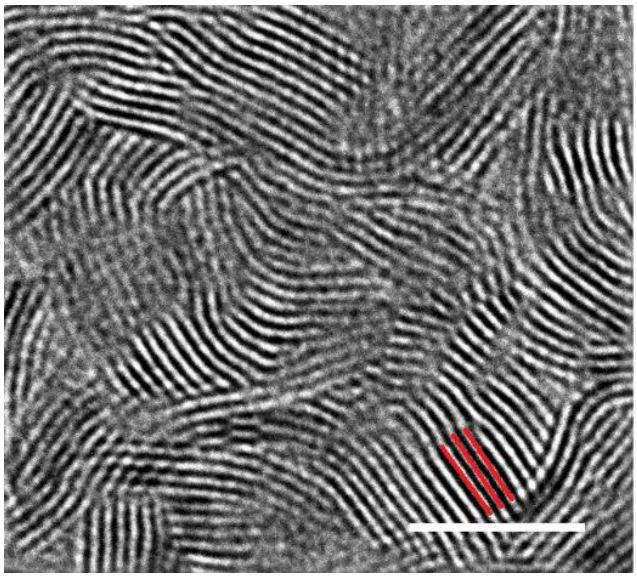

**Figure 3. High-resolution transmission electron micrograph of FLV-$MoS_2$ with >90% vertical-alignment $MoS_2$ thin film in the sample. The red lines correspond to the (002) basal lattice fringes, which indicate vertical alignment of domains within the film. Scale bar represents 10 nm.**

while low sulfur flux can result in MoS products with different stoichiometry. In order to investigate the effects of sulfur flux, three samples were prepared under optimal growth conditions with sulfur positioned to cooler areas in the furnace. In previous FLV-$MoS_2$ runs, the sulfur powder was typically placed 15.2 cm from the heating center of the furnace, positioned so that the center of the sulfur is over the inner edge of the insulator lip. In the FLV-$MoS_2$ sulfur position experiment runs, the sulfur was positioned at 16.5, 17.8, and 19.1 cm away from the heating center of the furnace as shown in Figure 4. Positioning the sulfur further outside the furnace led to improved photocatalytic performance results as observed in the 16.5 and 19.1 cm samples.

UV-Vis spectroscopy was used to characterize the FLV-$MoS_2$ as shown in Figure 5. The location of the peaks at around 620 and 670 nm within a representative sample are similar to those in spectrum found in the literature[7]. This doublet is caused by the spin-orbital splitting of the valence band inherent to $MoS_2$.[8] However, the absorbance values of the samples are higher across the entire spectrum compared to literature[7]. This difference in UV-Vis results may be due to the literature data measuring the reflectance while the UV-Vis measurements of this study does not account for reflectance. Taking the reflectance signal into consideration would reduce the absorbance values by increasing the effective transmittance through the sample.

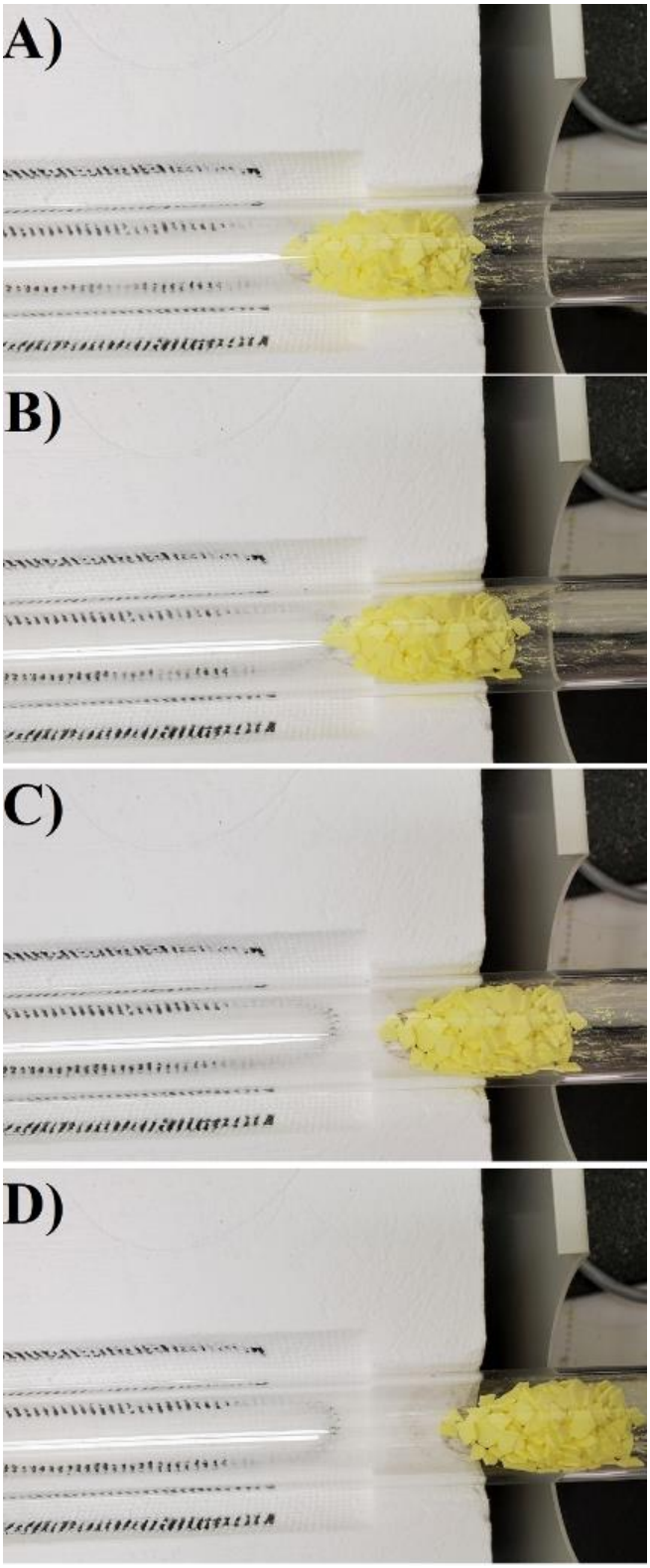


**Figure 4. Sulfur positioning with the center of the sulfur shifted to A) 15.2 cm, B) 16.5 cm, C) 17.8 cm, and D) 19.1 cm from the heating center of the furnace.**

**B. Photocatalytic Performance Results**

For the first three depositions, the FLV-$MoS_2$ photocatalytic performance results continued to show low biocidal efficacy (less than 1 log kill after 4 hours) and low $H_2O_2$ production (less than 0.5 μM $H_2O_2$ over 4 hours) while the literature[7] reports a 5 log kill and 2 μM $H_2O_2$ after 2 hours. The best $H_2O_2$ formation obtained from these depositions from a FLV-$MoS_2$ sample with 80% vertical-alignment was 0.8 μM produced after 4 hours. However, the improved performance was not reproducible and the performance of FLV-$MoS_2$ found in the literature is approximately 10 times higher than the current best results.

The $H_2O_2$ formation testing procedure was modified for a possible cause of the low $H_2O_2$ formation. The FLV-$MoS_2$ reaction mechanism requires oxygen to form ROS with a potential

consumption of oxygen at the FLV-$MoS_2$ active site interface during the photochemical reaction. Thus, the water was stirred during the light exposure to circulate oxygen to react at the $MoS_2$ active sites. The highest performing sample was placed on a stir plate to stir the DI water at 250 rpm. However, the stirring only increased the $H_2O_2$ production to 1 µM after 4 hours compared to 0.8 µM $H_2O_2$ obtained after 4 hours without stirring, which is lower than the literature[7] results of 2 µM formed after 2 hours.

Initial $H_2O_2$ formation results of the fourth deposition remained low at 0.4-0.5 µM produced over 4 hours. However, the sulfur positioning experiment samples showed significantly higher $H_2O_2$ formation rates with the sample at sulfur positions 16.5, 17.8, and 19.1 cm forming 1.5, 1.2, and 1.1 µM $H_2O_2$ at 4 hours, respectively. This significant increase in $H_2O_2$ formation brought the photocatalytic performance within approximately 17% of the FLV-$MoS_2$ in the literature[7]. Based on these results, biocidal efficacy testing was performed on the 16.5 and 19.1 cm samples. The 16.5 cm sample has a 0.5 log kill in 4 hours while the 19.1 cm sample has a 1.9 log kill in the same time period as shown in Figure 6. This notable improvement over the previous results indicates that our $H_2O_2$ formation measurements do not correlate with biocidal kill as the sample with lower $H_2O_2$ formed had a higher bacterial kill rate. This could be explained by the presence of contaminants that consume $H_2O_2$, resulting in low residual $H_2O_2$ measurements. This poor correlation between $H_2O_2$ formation and biocidal efficacy results indicates the need for biocidal efficacy testing on previous FLV-$MoS_2$ samples that were considered ineffective due to low $H_2O_2$ formation. Furthermore, attempts to reproduce the conditions of the 16.5 cm sample showed low $H_2O_2$ formation of 0.2-0.5 µM at 4 hours, but biocidal efficacy testing of the samples shows a 1.0 – 1.9 log kill in 4 hours. It is unclear why sulfur positioning

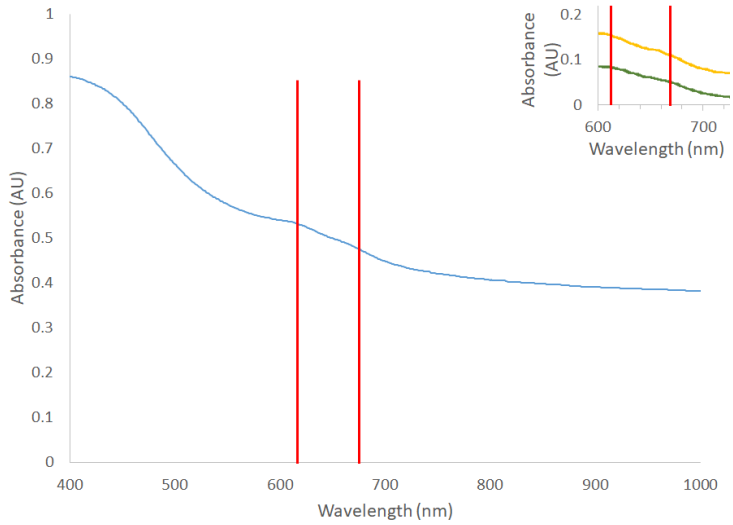


**Figure 5. UV-Vis absorbance spectrum of a representative 66-nm thick (estimated based on ref. 7) FLV-$MoS_2$ sample. The inset shows 40-nm thick (green) and 80-nm thick (yellow) FLV-$MoS_2$ recreated from UV-Vis data in literature (ref. 7). The broad peaks at ~620 and 670 nm, indicating the orbital splitting of the $MoS_2$ valence band, are shown in red.**

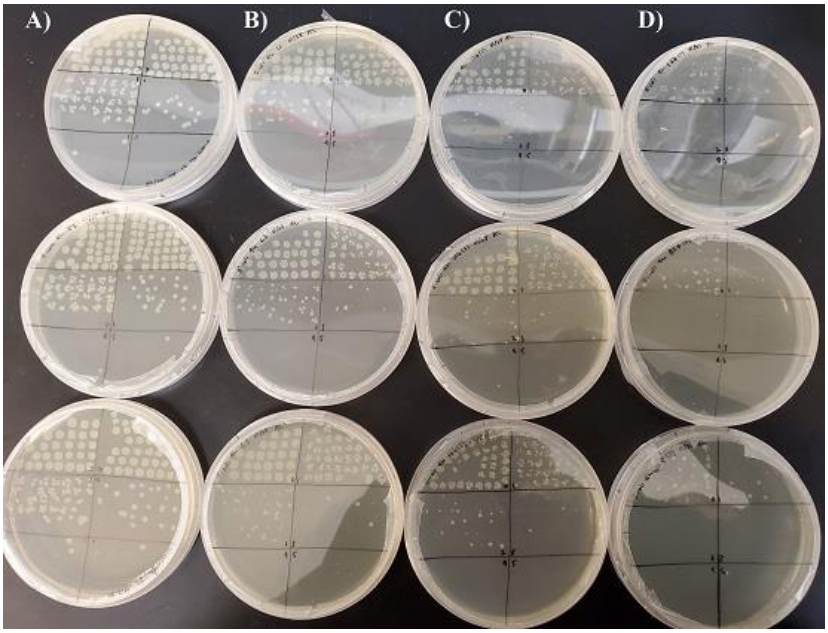


**Figure 6. Biocidal efficacy testing results at 4 hours of the A) dark control, B) light control, C) 16.5 cm sulfur position FLV-$MoS_2$ sample (1.5 µM $H_2O_2$ at 4 hours), and D) 19.1 cm sulfur position FLV-$MoS_2$ sample (1.1 µM $H_2O_2$ at 4 hours). CFU enumeration for each test condition ran in triplicate.**

sample of the same condition shows such broad variation in photocatalytic performance results. One possible explanation is that the $MoS_2$ films have poor adhesion to quartz, which will be discussed later.

### C. Gold Deposition

Previous research has reported an improvement of the FLV-$MoS_2$ photocatalytic performance by 2X with the deposition of 5 nm gold nanoparticles over the surface.[7] This is attributed to the trapping of the electron in the gold nanoparticle preventing the recombination of the electron and hole generated during the visible light activation.[7] Gold was deposited onto FLV-$MoS_2$ TEM grids and quartz slide samples (made at 500 °C and 30 Torr) by sputtering with IBS for 1, 2.2, and 5 minutes. The TEM images in Figure 7 show the increasing gold nanoparticle size in relation to sputtering time and their comparison to the control. The 1 minute sputtering run does not show a nanoparticle distribution in the TEM. When sputtering for 2.2 minutes, the gold nanoparticles are distinctly separated circles ranging 2-3 nm in diameter. At 5 minutes sputtering time, these nanoparticles begin to overlap and show a more oval shape with widths ranging 4-5 nm.

With the gold nanoparticle distributions observed, the $H_2O_2$ formation rate was measured in relation to the sputtering times. A twofold increase in $H_2O_2$ concentration was observed for the 5 minute gold sputtered sample over the control. An overall trend of increasing $H_2O_2$ concentration with increasing sputtering times is presented in Figure 8. Gold deposition experiments on FLV-$MoS_2$ were continued with sputtering times of 10.5-20 minutes, but the FLV-$MoS_2$ $H_2O_2$ formation rates degraded to levels below the unsputtered control.

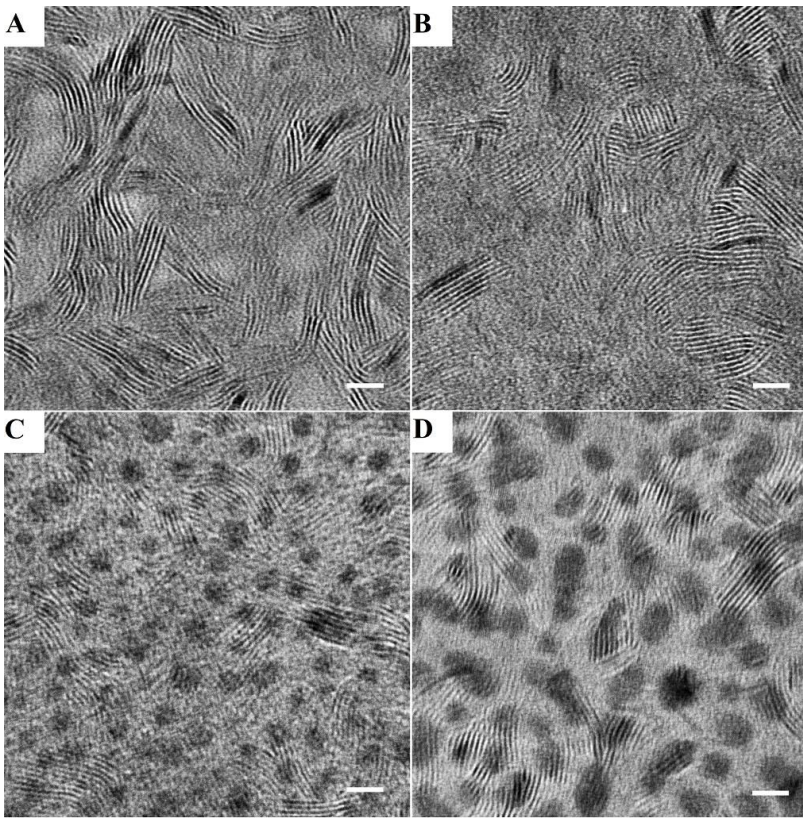


**Figure 7. High-resolution transmission electron micrographs showing A) unsputtered control FLV-$MoS_2$ made at 500 °C and 30 Torr along with FLV-$MoS_2$ made under the same conditions and sputtered for B) 1 min, C) 2.2 min, and D) 5 min at 500000X magnification. Scale bars represent 5 nm.**

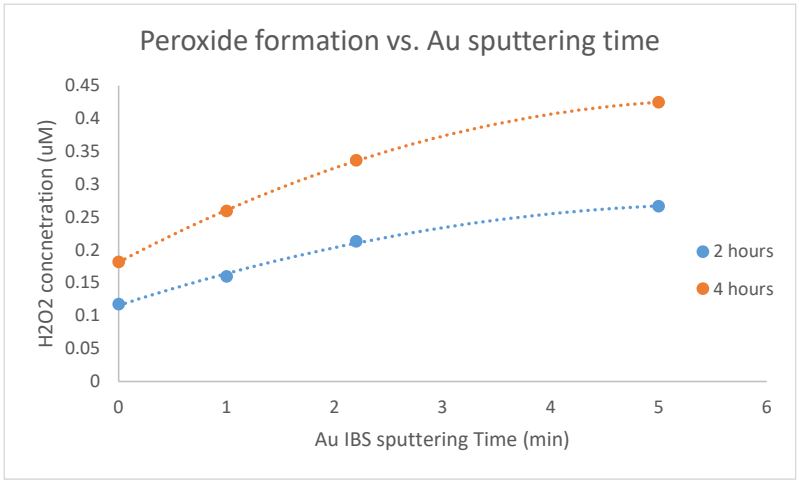


**Figure 8. Concentration of $H_2O_2$ formed in relation to gold sputtering times of 0, 1, 2.2, and 5 minutes with the $H_2O_2$ concentrations measured at 2 hours (blue) and 4 hours (orange). Linear-fit trendlines shown for each time point.**

An old sample from the second deposition Mo runs with a $H_2O_2$ formation rate of 0.8 µM in 4 hours was gold sputtered for 5 minutes, which caused the $H_2O_2$ formation rate to increase to 2.9 µM in 4 hours, the highest observed in our FLV-$MoS_2$ samples. However, the sample film showed visible delamination during the biocidal efficacy testing runs following this result. The delamination occurred throughout the entire film, which raised concern that the FLV-$MoS_2$ was not a viable long-term solution for water treatment applications.

**D. Film Delamination**

Previous FLV-$MoS_2$ samples made on quartz slides with the 13.8, 16.6, and 30.6 nm depositions under optimal growth conditions were immersed in water for two weeks. After the storage period, the samples were observed visually and under scanning electron microscopy (SEM) for film delamination. Two previous samples made on a glassy carbon and thermal oxide silicon wafer with the 12.6 nm deposition and three gold deposited samples on quartz slides from the 16.6 nm deposition were also immersed in water and observed for one week. All the FLV-$MoS_2$ samples on quartz slides showed visible film loss throughout the entire film, regardless of deposition thickness, within two weeks of immersion in water. This delamination showed no clear patterns of failure with areas of dark brown and light brown, indicating $MoS_2$ left on the chip, and clear areas of exposed quartz. Furthermore, fragments of $MoS_2$ film were found floating in the water after the experiment. Gold-deposited samples exhibited faster delamination as the $MoS_2$ films completely delaminate within one week, which may be caused by defects and damage to the surface of the FLV-$MoS_2$ surface during sputtering. In comparison to the quartz slide samples, the thermal oxide silicon wafer exhibited visible delamination on the edges where the chip rested on the quartz tube in the furnace, which indicates that the higher heat exposure to those edges may make the film more susceptible to delamination. In contrast to the samples made on quartz slides and the thermal oxide silicon wafer, the glassy carbon plate shows no loss in film with no film fragments found floating in the water and the surface color remained dark blue, which is characteristic of FLV-$MoS_2$ films.[6] These results were confirmed with SEM. In the quartz slide, the light and dark brown film left after water immersion shows exposed holes down to the quartz substrate as indicated by the bright areas of charging shown in Figure 9A. These holes are surrounded with a

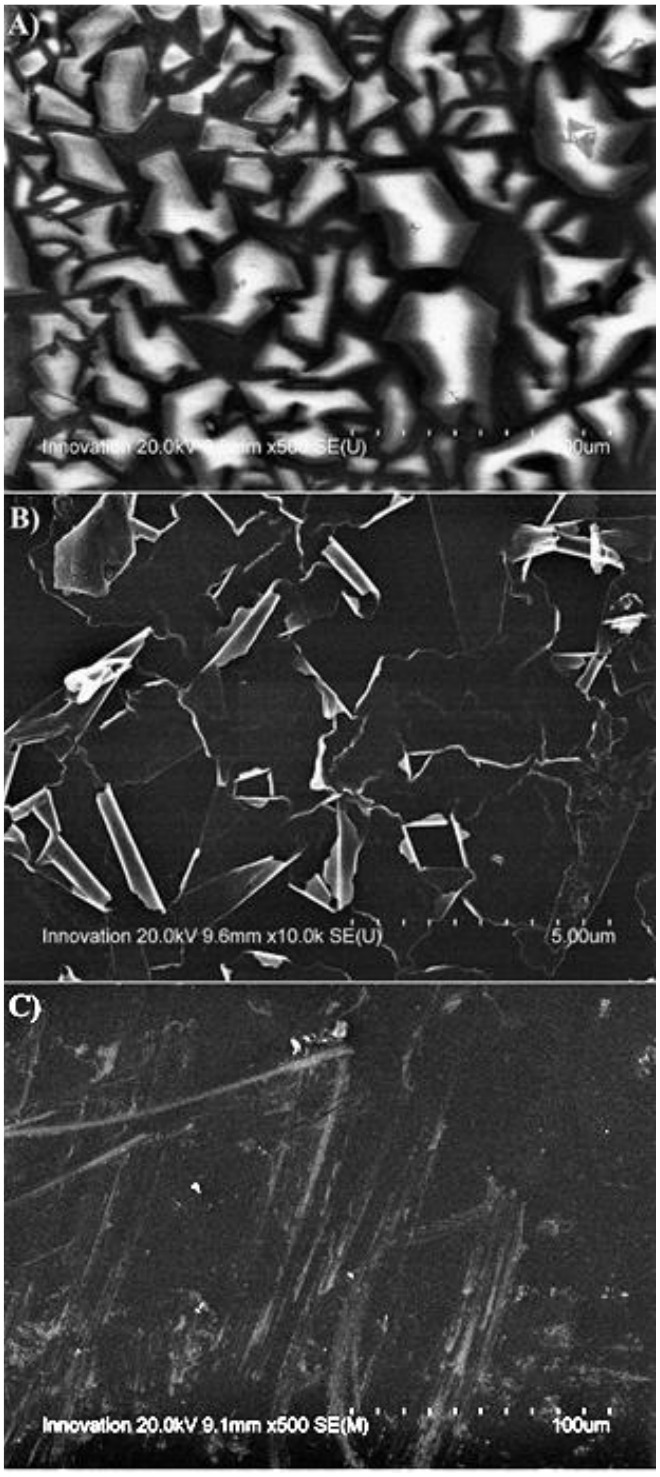


**Figure 9. Scanning electron micrographs of FLV-$MoS_2$ A) made with the 30.6 nm deposition on a quartz slide at 500X magnification, B) made with 12.3 nm deposition on the thermal oxide silicon wafer at 10,000X magnification, and C) made with the 12.3 nm deposition on the glassy carbon plate at 500X magnification.**

dark-light gray gradient, which can be explained by the observations of peeling and curling of the $MoS_2$ film as shown in the thermal oxide silicon wafer in Figure 9B. This film curling and liftoff indicates that the mechanism of failure in the $MoS_2$ films is the poor adhesion of the film to the silicon dioxide ($SiO_2$) substrate surface. The FLV-$MoS_2$ on glassy carbon sample only shows scratching from abrasion, likely from the handling of the sample, as shown in Figure 9C. However, this sample shows none of the same peeling behavior as those shown in Figures 9A and 9B. This may explain the variations in the FLV-$MoS_2$ sample photocatalytic performance results as the films are failing during the testing. Based on these early delamination results, glassy carbon substrates show better adhesion for FLV-$MoS_2$ and can allow for long-term disinfection while underwater. Continuing water immersion studies of FLV-$MoS_2$ on glassy carbon will verify these findings.

## IV. Future Work

Continuing studies into the aging of the Mo films, biocidal efficacy testing of previous samples, and the delamination of FLV-$MoS_2$ films over glassy carbon in water will be carried out to better understand how the FLV-$MoS_2$ performance is affected. In order to improve the photocatalytic performance of FLV-$MoS_2$ and show its viability, a final deposition of 50-nm thick Mo film will be carried out on glassy carbon substrates. FLV-$MoS_2$ reactions will be done with the sulfur positioned at 15.2 cm and 16.5 cm from the heating center along with other positions further outside the furnace and tested for biocidal efficacy. The goal of this future work is to obtain a reproducible FLV-$MoS_2$ process with greater than a 2 log kill in 1 hour and no film failure under running conditions for one year. If successful, FLV-$MoS_2$ can prove to be a suitable solution for the disinfection of potable water systems.

## V.Conclusion

A significant improvement in the vertical-alignment of FLV-$MoS_2$ was observed by using thicker Mo film layer. Additionally, the position of the sulfur at the inlet of the furnace also affected the performance. Positioning the sulfur 19.1 cm from the middle of the furnace produced the best performance in biocidal efficacy. Further, it became clear during repeated runs that our $H_2O_2$ testing did not predict biocidal efficacy where samples with high $H_2O_2$ formation had poor biocidal efficacy and vice versa. The use of 4-5 nm diameter gold nanoparticle decoration produced a two-fold increase in the $H_2O_2$ formation, however, biocidal efficacy testing was not performed due to film delamination. This delamination occured within 1-2 weeks and is attributed to poor adhesion of the FLV-$MoS_2$ to the $SiO_2$ of the quartz and thermal oxide silicon substrates. However, the glassy carbon substrate showed no film delamination after a week of immersion, which indicates that glassy carbon may be a viable substrate for FLV-$MoS_2$ growth.

## Acknowledgments

The authors acknowledge with special thanks to John Hogan and Asif Rahman for their tutelage in all things biological, the AES Water Project for funding this research, and Desheng Kong for guidance on FLV-$MoS_2$ growth.

## References

[1]World Health Organization, "Alternative drinking-water disinfectants: bromine, iodine and silver," 2018.

[2]Punyani, S., Narayana, P., Singh, H., and Vasudevan, P., "Iodine based water disinfection: A review," *Journal of Scientific & Industrial Research*, Vol. 65, 2006, pp. 116-120.

[3]Helme, A. J., Ismail, M. N., Scarano, F. J., and Yang, C. L., "Bactericidal efficacy of electrochemically activated solutions and of commercially available hypochlorite," *British Journal of Biomedical Science*, Vol. 67, No. 3, 2010, pp. 105-108.

[4]Pathak, Satya P., and Gopal, K., "Evaluation of bactericidal efficacy of silver ions on Escherichia coli for drinking water disinfection," *Environmental Science and Pollution Research*, Vol. 19, No. 6, 2012, pp. 2285-2290.

[5]Slote, B., Salley, E., Carr, D., Kimble, M., & Adam, N., "Silver Ion Biocide Delivery System for Water Disinfection.," *46th International Conference on Environmental Systems*, July 10-14, 2016. AIAA Paper # 2016-136.

[6]Kong, D., Wang, H., Cha, J. J., Pasta, M., Koski, K. J., Yao, J., and Cui, Y., "Synthesis of MoS2 and MoSe2 Films with Vertically Aligned Layers," *Nano Letters*, Vol.13, No. 3, 2013, pp. 1341-1347.

[7]Liu. C., et al., "Rapid water disinfection using vertically aligned MoS2 nanofilms and visible light," *Nature Nanotechnology*, Vol. 11, No. 12, 2016, pp. 1098-1104.

[8]Jung, Y., Shen, J., Liu, Y., Woods, J. M., Sun, Y., and Cha, J. J., "Metal Seed Layer Thickness-Induced Transition From Vertical to Horizontal Growth of MoS2 and WS2," *Nano Letters*, Vol. 14, No. 12, 2014, pp. 6842-6849.

[9]Delzeit, L., and Vance, J. R., "BioMoSS: Biocidal MoS2 for disinfection of spacecraft potable water systems," *49th International Conference on Environmental Systems*, July 7-11, 2019. AIAA Paper # 2019-124.

[10]Wolff, S. P., "Ferrous ion oxidation in presence of ferric ion indicator xylenol orange for measurement of hydroperoxides," *Methods in Enzymology*, Vol. 233, 1994, pp. 182-189.

[11]Pirmohamed, Talib, et al., "Nanoceria Exhibit Redox State-Dependent Catalase Mimetic Activity," *Chemical Communications*, Vol. 46, No. 16, 2010, pp. 2736-2738.

[12]Thomas, P., Sekhar, A. C., Upreti, R., Mujawar, M. M., & Pasha, S. S., "Optimization of Single Plate-Serial Dilution Spotting (SP-SDS) with Sample Anchoring as an Assured Method for Bacterial and Yeast Cfu Enumeration and Single Colony Isolation from Diverse Samples," *Biotechnology Reports*, Vol. 8, 2015, pp. 45-55.

[13]Kong, D., "Re:NASA interest in FLV-MoS2," Message to John Abdou. 9 January 2020. E-mail.

[14]Müller, R., Yulin, S., Naujok, P., Kaiser, N., and Tünnermann, A., "Optical Properties and Oxidation Resistance of Different Transition Metals for Soft X-Ray and EUV Applications." *Thin Solid Films*, Vol. 624, 2017, pp. 1-6.